International Journal of Biological Macromolecules 283 (2024) 137664

Contents lists available at ScienceDirect

International Journal of Biological Macromolecules

journal homepage: www.elsevier.com/locate/ijbiomac

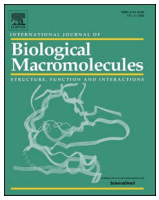

Fabricating dehydrated albumen with a novel variable frequency ultrasonic drying method: Drying kinetics, physiochemical and foaming characteristics

Vedant Mundada [a], Gulsah Karabulut [b], Ragya Kapoor [a], Amir Malvandi [c], Hao Feng [a,d,*]

[a] Department of Food Science and Human Nutrition, University of Illinois at Urbana-Champaign, Urbana, IL 61801, USA
[b] Department of Food Engineering, Faculty of Engineering, Sakarya University, 54187 Sakarya, Türkiye
[c] Department of Agricultural and Biological Engineering, University of Illinois Urbana-Champaign, Urbana, IL 61801, USA
[d] Department of Family and Consumer Sciences, North Carolina A&T State University, Greensboro, NC 27411, USA

ARTICLE INFO

Keywords:
Albumen
Drying kinetics
Ultrasonic drying
Functional properties

ABSTRACT

Albumen, primarily composed of ovalbumin, is a vital, nutrient-rich ingredient in the food industry. Drying is a critical step in low-water-activity albumen powder production, allowing extended shelf-life and reduced costs in handling, transportation, and storage of albumen products. Traditional drying methods, such as spray drying (SD) and hot air drying (HAD), often degrade albumen. This study explores variable frequency contact ultrasonic drying (CUD) as a novel and green alternative, operating at a central frequency of 20 kHz with sound amplitudes of 0 %, 40 %, and 60 %, and temperatures of 40 °C and 60 °C. The drying kinetics, physical, and foaming properties of CUD-dried albumen proteins were compared with those of hot-air-, spray-, and freeze-dried (FD) samples. Compared to HAD, CUD significantly enhanced the drying process, as evidenced by a 240 % increase in effective moisture diffusivity, a 66–78 % reduction in activation energy (Ea), and a 27 % reduction in drying time. Moreover, CUD maintained higher protein integrity, evident from a 24–35 % decrease in enthalpies, more β-turn and random coil structures, and increased free sulfhydryl groups. Notably, CUD at 40 °C significantly improved foaming capacity by 88 %, and at 60 °C, it enhanced foaming stability by 34 %, outperforming other drying methods. Protein solubility of CUD-albumen was improved by 10–12 % compared to HAD and was slightly better than FD. CUD-albumen showed a brighter color with a 26 % lower browning index than the HAD samples. Overall, CUD emerges as an effective and sustainable method for drying high-protein materials, ensuring high-quality albumen powders.

1. Introduction

The importance of eggs in the human diet is unmatched. Eggs are affordable and nutrient-packed, rich in proteins or albumen, fats, and minerals. Recent times have seen a significant rise in the demand for proteins, leading to a remarkable 203.2 % increase in the production of eggs over the past 35 years [1,2]. Albumen is extensively utilized in the food industry due to their versatile properties, such as gelling, foaming, and thickening, which are crucial in various sectors, including bakeries [3].

The nutrient-laden albumen has approximately 88 % water, making it an excellent medium for microbial growth. This makes albumen prone to spoilage, leading to a short shelf life of up to 4 days in the refrigerator [4]. Researchers have explored various techniques to address this issue, including pasteurizing liquid albumen, refrigerating, applying surface coatings, and freezing [5]. Among the various preservation techniques, drying has been extensively employed as a primary method to extend the shelf life of albumen. The removal of water from the food matrix offers several advantages, including facilitating transportation by reducing weight, managing surplus production, and addressing supply shortages [6].

Drying is one of the most important processing methods, accounting for 7–15 % of the total industrial energy consumption. Traditional drying methods, such as spray drying (SD), hot air drying (HAD), and freeze drying (FD), consume high quantities of energy with an efficiency of only 25–50 %, making them less efficient for drying albumen or egg white. Among the possible methods for drying, the most widely used methods are SD and HAD. However, both SD and HAD involve exposing

* Corresponding author at: Department of Food Science and Human Nutrition, University of Illinois at Urbana-Champaign, Urbana, IL 61801, USA.
E-mail address: hfeng@ncat.edu (H. Feng).

https://doi.org/10.1016/j.ijbiomac.2024.137664
Received 10 August 2024; Received in revised form 10 November 2024; Accepted 13 November 2024
Available online 17 November 2024
0141-8130/© 2024 Published by Elsevier B.V.

the material to high heat, causing undesired changes. Due to this heat exposure, various sulfur and apolar amino acids are formed during drying [7]. Ovalbumin and ovotransferrin are the major proteins in albumen, with denaturation temperatures of 84 °C and 65 °C, respectively [8]. Exposure to temperatures above the denaturation threshold induces structural alterations in proteins at the tertiary and quaternary levels, significantly impairing the functional properties of albumen [8,9]. Freeze drying, on the other hand, involves the removal of moisture at low temperatures under reduced pressure via a sublimation pathway. The low-temperature method produces arguably the best quality dried product. However, the process requires long drying times and is very cost and energy intensive. The drawbacks of existing methods have spurred research into alternative and new drying technologies [10,11]. In recent years, non-thermal technologies like ultrasound (US) have gained popularity and applications in the food industry [12]. Ultrasound is used not only for food analysis (e.g., high frequency, low intensity ultrasound) but also in assisted novel processing methods (e.g., low frequency, high intensity) [9]. Power ultrasound, with sound intensity of over 1 W/cm^2, has been studied for use in areas of emulsification [13], enzyme and microbial inactivation [14], extraction [15], crystallization [16] and drying [17]. In drying, US improves drying kinetics, reduces drying times, and preserves the nutritional and functional properties of food materials [18].

In this study, we examined an innovative, energy-saving, and green approach called contact ultrasonic drying (CUD) for processing albumen. This method utilizes the transmission of acoustic energy to provoke specific physical actions within a food biopolymeric matrix. Notably, it causes liquids to move in one direction, following the path of the sound waves, which significantly enhances mass transfer activities such as moisture removal [19]. Additionally, when there is a high moisture content, acoustic cavitation occurs, creating a mist over the drying product's surface [20]. This allows for the removal of water as mist without a phase change, facilitating swift drying with reduced energy consumption. Using this technology, Malvandi et al. [21] reported a 46 % reduction in drying times and approximately 50 % reduction in activation energies for CUD of distillers dried grains. Similarly, employing CUD for pea protein suspensions resulted in a 55 % decrease in drying time compared to HAD [18]. Moreover, the average effective moisture diffusivity in the CUD process was observed to be 325 % higher than in HAD. This technique not only enhanced the drying efficiency but also maintained a high quality in the dried products, showcasing CUD as an energy-efficient alternative to traditional drying methods.

Our study aims to utilize novel CUD for heat-sensitive, protein-rich albumen and to compare the drying kinetics, diffusivities, activation energies, and protein quality parameters to those of HAD, SD, and FD. The drying curves were fitted to semi-empirical models, and the fitting parameters were evaluated. Our hypothesis is that the CUD process enhances the drying efficiency and improves the drying process variables, providing a sustainable drying method. The quality and functional properties, including solubility, microstructure, color, sulphydryl group content, and foaming capacities of albumen obtained from the CUD process, were compared to those produced by SD, FD, and HAD, which are more commonly used in the industry.

2. Materials and methods

2.1. Raw materials and chemicals

Fresh eggs were purchased from a local market (Urbana-Champaign, USA). The albumen were separated from the yolks, and the chalazae were removed. The albumen were gently stirred using a magnetic stirrer to avoid bubble formation, ensuring uniform and proper flowing properties. These liquid albumen were then used for drying. The chemicals used in the study were all purchased from Sigma-Aldrich (St. Louis, MO, USA).

2.2. Drying of albumen and moisture content

This study employed 4 different drying techniques to obtain albumen powders, i.e., CUD, HAD, SD, and FD techniques. The properties and kinetics of CUD were then compared against that of the HAD.

2.2.1. Contact ultrasound drying (CUD) and hot air drying (HAD)

The CUD and HAD of albumen were performed using a novel custom-built system as described by Malvandi et al. [17]. The system includes a variable frequency US generator with a central frequency of 20 kHz, capable of producing waves with a maximum power of 1000 W, as illustrated in Fig. 1. The drying surface is a rectangular metallic plate that vibrates at variable ultrasonic frequency. A multi-frequency, multimode, and modulated (MMM) ultrasound generation method was used in the system. The MMM module produces digital signal to synchronously excite a number of vibrating modes including harmonics and sub-harmonics of acoustic loads, thereby creating a uniform vibration over the drying surface. Hot air was forced to flow above the vibrating plate at a speed of 5 m/s. Compressed air was used to cool down the heating piezoelectric transducer. The liquid albumen were uniformly spread over the vibrating rectangular surface of the system with a uniform thickness of 1 mm, 40 % and 60 %, and at temperatures of 40 °C (CUD40A40: 40 % amplitude; CUD40A60: 60 % amplitude) and 60 °C (CUD60A40: 40 % amplitude and CUD60A60: 60 % amplitude). The US was applied with a 3 s on and 1 s off pulse time to reduce heating and energy consumption during drying. HAD was performed using the same unit without turning on ultrasound. HAD was carried out at 40 °C (HAD40) and 60 °C (HAD60), similar to CUD. Drying continued until a final moisture content of 7–9 % (wet basis) was reached.

2.2.2. Spray drying (SD)

A lab scale spray dryer (Buchi Corporation B-290, Switzerland) was used for SD of liquid albumen. An inlet air temperature of 160 °C with the co-current flow was used, with a feed flow rate of 6–8 mL/min in a two-fluid nozzle. The outlet temperature varied between 70 and 75 °C. The aspirator was set at 100 % with a gauge pressure of −65 ± 5 mBar [22,23].

2.2.3. Freeze-drying (FD)

The FD of liquid albumen was done at −50 °C and 0.08 mBar using the freeze dryer (Labconco Corporation, USA). FD-albumen powders were then ground using a benchtop coffee grinder for 30 s to obtain a homogenous powder. All dried samples were stored in airtight containers at −2 °C. During the drying process for CUD and HAD, samples weighing approximately 1 g were periodically obtained for moisture content analysis. Moisture content was measured using a halogen moisture content analyzer (HR83, Mettler Toledo, USA). The periodic measurement of the moisture content during the drying process was used to create the drying curves.

2.2.4. Drying variables and rate

Moisture ratio (MR) is a dimensionless number widely used to describe and analyze a drying process. It indicates the amount of water present compared to the initial amount at the start of drying [17]. The moisture ratio was calculated using Eq. (1):

$$MR(\mathrm{t}) = \frac{MC_{db}(t) - MC_{db}(eq)}{MC_{db}(i) - MC_{db}(eq)} \quad (1)$$

where $MC_{db}(t)$ is the moisture content at time t, $MC_{db}(i)$ refers to the initial moisture content (dry basis), and $MC_{db}(eq)$ is the equilibrium moisture content (dry basis).

The drying rate (DR, min^{-1}) was calculated using Eq. (2):

$$DR(t) = \frac{MC_{db}(t) - MC_{db}(t + \Delta t)}{\Delta t} \quad (2)$$

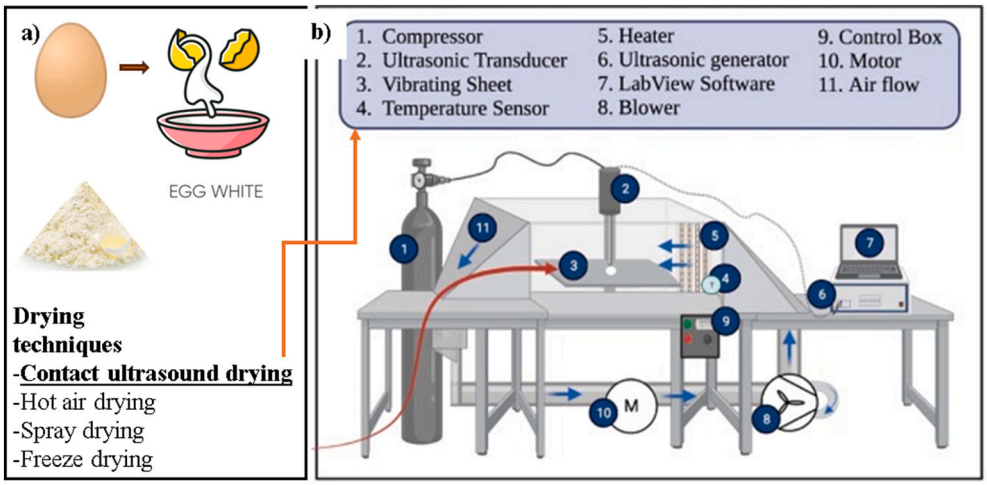

Fig. 1. Schematic of the MMM contact ultrasonic dryer from Kapoor et al. [9].

where $MC_{db}(t)$ is the moisture content at time t (dry basis), $MC_{db}(t+\Delta t)$ is the moisture content at $t+\Delta t$ (kg water/kg dry matter), and t is the drying time (s).

A number of semi-empirical models were compared and fitted to the drying curves (Table 1). The constants for the models were found using the Levenberg–Marquardt algorithm [24]. The coefficient of determination (R^2), residual sum of squares (RSS), and the chi-squared values (χ^2) were utilized to evaluate the performance of the models, according to Eqs. (3)–(5).

$$R^2 = 1 - \frac{\sum_{i=1}^{N}\left(MR_{exp,i} - MR_{pre,i}\right)^2}{\sum_{i=1}^{N}\left(\overline{MR_{exp,i}} - MR_{pre,i}\right)^2} \tag{3}$$

$$RSS = \sum_{i=1}^{N}\left(MR_{exp,i} - MR_{pre,i}\right)^2 \tag{4}$$

$$\chi^2 = \frac{\sum_{i=1}^{N}\left(MR_{exp,i} - MR_{pre,i}\right)^2}{N-n} \tag{5}$$

where $MR_{exp,i}$ and $MR_{pre,i}$ represent the experimental and the predicted dimensionless moisture ratios for a particular observation (i), respectively. N refers to the total number of observations, while n is a constant.

The coefficient of determination (R^2) measures how well the experimental data fits the regression line, ranging from 0 to 1, with values close to 1 indicating a better fit. The residual sum of squares (RSS) quantifies the variability of the regression function. The reduced chi-squared value, calculated by dividing the RSS by the degrees of freedom, represents the ratio of experimental to theoretical variance. Lower RSS and chi-squared values indicate a superior fit.

Table 1
Semi-empirical models used for fitting of the egg white drying curves.

Model name	Equations
Lewis Model [37]	$MR = exp(-kt)$
Page Model [64]	$MR = exp(-kt^n)$
Henderson and Pabis Model [65]	$MR = a \times exp(-kt)$
Two-Term Model [66]	$MR = a \times exp(-kt) + b \times exp(-mt)$
Approximation and Diffusion Model [67]	$MR = a \times exp(-kt) + (1-a) \times exp(-kbt)$
Logarithmic Model [68]	$MR = a \times exp(-kt) + b$
Two-term Exponential Model [69]	$MR = a \times exp(-kt) + (1-a) \times exp(-kat)$

2.2.5. Effective moisture diffusivity and activation energy

The falling rate drying involves the internal mass transfer controlling the process and the Fick's second law of diffusion mathematically describes it. Fick's second law of diffusion is used to explain the diffusion in systems that have changing concentrations. This law explains diffusion in systems with changing concentrations and provides analytical solutions under three assumptions (i) negligible shrinkage during the process, (ii) surface and hot convective air are under a condition of thermal equilibrium, and (iii) diffusivity is constant [25]. The law can be expressed as in Eqs. (6) and (7):

$$\frac{\partial(MC_{db})}{\partial t} = D_{eff}\frac{\partial^2(MC_{db})}{\partial y^2} \tag{6}$$

$$MR = \frac{8}{\pi^2}\sum_{n=1}^{\infty}\frac{1}{(2n-1)^2}\,exp\left[-\frac{(2n-1)^2\,\pi^2\,D_{eff}\,t}{4L^2}\right] \tag{7}$$

where D_{eff} (m^2/s) is effective diffusivity, t (s) is time, and L is the half-thickness of the samples (m).

This equation was solved using MATLAB software (MathWorks, USA) to determine the effective moisture diffusivities at various times during the drying process. The average effective diffusivity (m^2/s) was calculated as Eq. (8) [26]:

$$D_{eff,avg} = \frac{\int D_{eff} MC_{db}\, dMC_{db}}{\int dMC_{db}} \tag{8}$$

2.3. Albumen quality and functional attributes

2.3.1. Color parameters

The color of the final albumen powder was measured using a CIE *Lab** color scale with a reflectance-type colorimeter (LabScan XE, Hunter Associates Laboratories, USA). The *L** *values* indicate brightness (0 to 100, with higher values indicating brighter colors). The *a** axis ranges from green (−) to red (+), and the *b** axis ranges from blue (−) to yellow (+). After standardizing the colorimeter, readings for albumen powders were taken in triplicates at room temperature. The *L**, *a**, and *b** values were used to calculate the browning index (BI) using Eqs. (9) and (10) [27]. The (BI) is a parameter that indicates the discoloration and browning the product has undergone during the drying process.

$$BI = \frac{100(x-0.31)}{0.17} \tag{9}$$

$$x = \frac{a^* + 1.75L^*}{5.645L^* + a^* - 3.012b^*} \tag{10}$$

where BI, L^*, a^*, and b^* are browning index, lightness, redness/greenness, and yellowness/blueness, respectively.

2.3.2. Densities, flow indices, and water activity

The bulk density (BD), tapped density (TD), Hausner ratio (HR), and Carr's compressibility index (CI) of the albumen powders were evaluated using the method described by Kapoor and Feng [28]. BD was determined by dividing the mass of the albumen powder by its volume in a graduated cylinder. To calculate TD, the powder was tapped 200 times in a glass cylinder, and the volume after settling was measured and then divided by the weight of powder. Both HR and CI were derived from the calculated values of bulk and tapped densities [31]. The water activity (a_w) of the final albumen powders was measured using a water activity meter (Aqualab 4TE Stand Alone, Nelson Jameson, USA).

2.3.3. Scanning electron microscopy (SEM)

The surface morphology of the particles was observed using a SEM (S-4800 SEM, Hitachi, Ltd., Tokyo, Japan). The dried albumen were placed onto a non-magnetic sample holder using a two-sided carbon adhesive tape. Loose particles were removed from the sample using compressed air to shake off any particles not adhered to the tape. Albumen is a non-conductive material when it comes to electricity, hence the samples were coated with a gold-platinum layer by the sputter coating for 40 s. Images were observed and captured at various magnifications using an accelerating voltage of 15 kV.

2.3.4. Circular dichroism spectroscopy (CD)

The secondary structure of albumen powders was determined by performing CD spectroscopy (Jasco, 1500, USA) at 25 °C [29]. The resultant sample spectrum was subsequently analyzed using Beta Structure Selection (BeStSel) (https://bestsel.elte.hu/index.php) to estimate the secondary structure of proteins.

2.3.5. Fourier-transform infrared spectroscopy (FTIR)

The FTIR spectra (PerkinElmer, Two 100521, USA) of albumen powders were analyzed from a range of 450 cm^{-1} to 4500 cm^{-1}. Each spectrum was generated by acquiring 16 scans with a resolution of 4 cm^{-1}. The peaks of the resulting spectra were analyzed to observe the changes in Amide A, I, II, and III peaks.

2.3.6. Differential scanning calorimetry (DSC)

A total of 10 mg of albumen powders and 10 μL of distilled water were sealed in a hermetically closed DSC aluminum pan and allowed to equilibrate at room temperature for 6 h. Using a DSC (TA Instruments, Q2000, USA), the pans were heated from 30 °C to 120 °C at a rate of 10 °C/min under a nitrogen purge of 50 mL/min, with an empty pan serving as the reference [30]. DSC results were analyzed using TA Universal Analysis 2000 software Version 4.5A (TA Instruments, USA).

2.3.7. Soluble protein content

Protein solubility of albumen powders was measured using the Bradford method [31]. Albumen solutions (10 mg/mL in distilled water) were mixed for 1 h, then centrifuged at 1450*g* for 10 min. To 1 mL of the resulting supernatant, 50 μL of Bradford reagent was added and incubated in the dark for 10 min. Absorbance was measured at 595 nm with a UV–Vis spectrophotometer (Spectronic Genesys 5, Thermo Scientific, USA). A standard calibration curve was created using bovine serum albumin ($R^2 = 0.997$), and solubility was calculated as the ratio of soluble to total proteins.

2.3.8. Total and free sulphydryl content

The total and free sulphydryl contents were determined using modified Ellman's reagent method, as described by Kapoor and Feng [32]. Two buffer solutions were prepared: Buffer I for free sulphydryl measurement contained 0.086 M Tris, 0.09 M Glycine, and 4 mM EDTA; Buffer II for total sulphydryl measurement included Buffer I plus 8 M Urea and 0.5 % sodium dodecyl sulfate. Albumen powder (0.5 g) was dissolved in 10 mL of each buffer and shaken for 1 h before centrifugation at 1450*g* for 15 min. To 1 mL of the supernatant, 10 μL of Ellman's reagent was added, and the mixture was incubated in the dark for 15 min. Absorbance was measured at 412 nm using a UV–Vis spectrophotometer (Spectronic Genesys 5, Thermo Scientific, USA). The contents of free sulphydryl (SH) and total sulphydryl (SS) were calculated using Eqs. (11) and (12), respectively.

$$SH\ content\left(\frac{\mu mol}{g}\right) = \frac{73.53 \times A \times D}{C} \tag{11}$$

$$SS\ content\left(\frac{\mu mol}{g}\right) = \frac{Total\ SH\ content - Free\ SH\ content}{2} \tag{12}$$

where A, D, and C were absorbance at 412 nm, dilution factor, and concentration of the sample (50 mg/mL), respectively.

2.3.9. Foaming properties

Foaming capacity and stability were assessed with slight modifications to the method described in Lan et al. [33]. Initially, 0.4 g of dried albumen powder was mixed with 20 mL of distilled water in a beaker. The mixture was homogenized (IKA, T-25 Wilmington, USA) at 10,000 rpm for 2 min. The foamed suspension was transferred to a graduated cylinder to measure the initial foamed volume. The foam was allowed to settle at room temperature, and the volumes were recorded at 30, 60, 90, and 120-mins intervals. Foaming capacity (FC) and stability (FS) were calculated using Eqs. (13) and (14), respectively.

$$FC\ (\%) = \frac{V_f - V_i}{V_i}\ x\ 100 \tag{13}$$

$$FS\ (\%) = \frac{V_t - V_i}{V_f - V_i}\ x\ 100 \tag{14}$$

where V_i (mL), V_f (mL), and V_t (mL) are the initial volume, initial foamed volume, and foamed volume at time intervals of 30, 60, 90, and 120 min.

2.4. Statistical analysis

The experiments were carried out in triplicates and values were reported as mean ± standard deviation. The statistical analysis was done using OriginPro software (Origin Pro, Version Number 2021b. OriginLab Corporation, Northampton, MA, USA). To determine the significant differences between means, the Tukey test with One-way ANOVA was employed at a significance level of $p < 0.05$.

3. Results and discussion

3.1. Drying curves and semi-empirical modeling

Drying data were fitted to seven semi-empirical models listed in Table 1, with fitting statistics presented in Table S1. All models showed a good fit, achieving R^2 values close to 1, along with low RSS and χ^2 values. The Page and Lewis models were particularly effective, both yielding high R^2 values above 0.99 and low RSS and χ^2 values. Models with fewer parameters are preferable for describing drying conditions [34]. The Page model, an enhanced version of Newton's model, includes a dimensionless model constant (n) along with the drying rate constant (k), minimizing errors found in the original Newton model [35]. Çalışkan et al. [34] also found the Page model to provide a good fit for drying albumen.

The Page model parameter k offers valuable insights into drying rate kinetics and allows for the comparison of different drying conditions. A higher k value indicates faster drying rates and shorter processing times [34]. The application of ultrasound increases k, as evidenced by 30 %

and 89 % increases at 40 % and 60 % amplitude at 40 °C, and 50 % and 124 % increases at 60 °C. These increases signify reduced drying times with ultrasound, which agrees with the report of Huang et al. [12]. Higher temperatures also result in higher *k* values under the same ultrasound conditions, confirming Onwude et al.'s findings [35]. Table S1 illustrates the significant impact of temperature and ultrasound amplitude on *k* values.

Drying curves were plotted and fitted to the Page model (Fig. 2a and b), revealing two main sections: the initial period and the falling rate period [17]. The initial period involves rapid surface moisture loss and

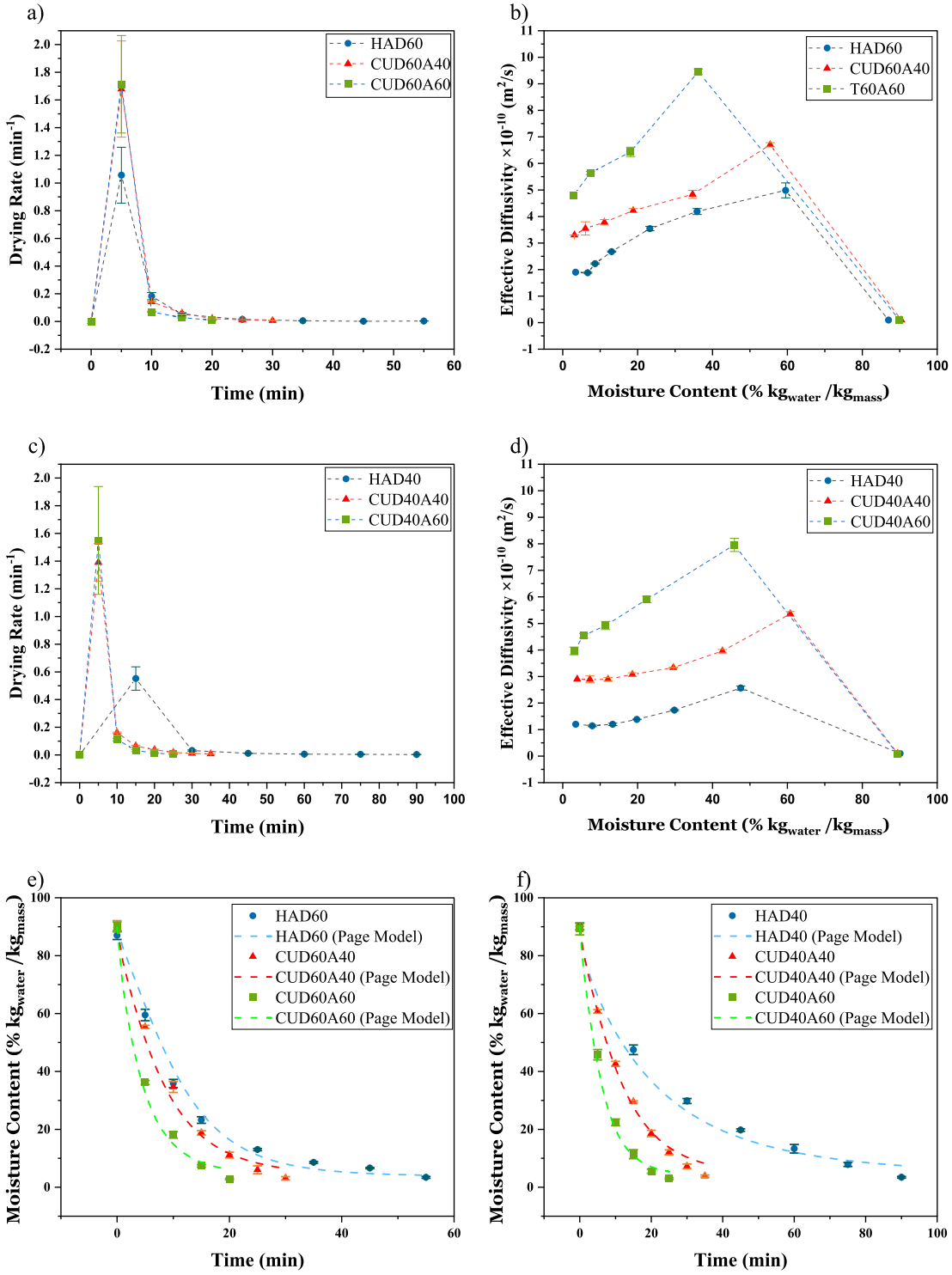

Fig. 2. Comparing drying curves, drying rates and effective moisture diffusivities for various CUD and HAD egg whites (EW). a) drying rate curves for samples dried at 60 °C, b) effective diffusivities for samples dried at 60 °C, c) drying rate curves for samples dried at 40 °C, d) effective diffusivities for samples dried at 60 °C, e) drying curves for samples dried at 60 °C, and f) drying curves for samples dried at 60 °C.
HAD40 = Hot Air Drying (HAD) at 40 °C, HAD60 = HAD at 60 °C; CUD40A40 = Contact Ultrasound Drying (CUD) at 40 °C and 40 % amplitude, CUD60A40 = CUD at 60 °C and 40 % amplitude, CUD40A60 = CUD at 40 °C and 60 % amplitude, CUD60A60 = CUD at 60 °C and 60 % amplitude., FD = Freeze Drying, SD = Spray Drying.

high drying rates (Fig. 2c and d), which is attributed to the removal of surface moisture. As the surface dries, internal moisture must travel through a porous matrix to reach product surface, leading to a reduction in drying rate. Lower moisture content decreases the drying rate because of smaller vapor pressure differences [36]. Increasing the temperature from 40 °C to 60 °C reduced drying time by ~39 %, similar to the findings in drying of tea [37], figs. [38] and distillers dried grain [17].

CUD reduced drying time and increased drying rate compared to HAD, with greater reductions at higher amplitudes and lower temperatures (Fig. 2a and b). At 40 °C, US at 40 % and 60 % amplitudes reduced drying times by 61 % and 72 %, respectively, and at 60 °C, by 45 % and 63 %. Gallego-Juárez et al. [39] also reported a similar reduction in the effectiveness of ultrasound with increasing temperatures. At a higher temperature, there is a greater ultrasound impedance mismatch between the vibrating plate and the samples. Thus, less acoustic energy is coupled into the sample at a higher temperature, and the contribution of ultrasound becomes less pronounced compared to drying at a lower temperature. The accelerated drying with ultrasound can be attributed to two factors. First, the longitudinal sound transmitted in food sample is comprised of a series of compressions and rarefactions moving in the direct of wave prorogation. This unidirectional wave prorogation can induce pressure waves that can push internal moisture to the surface thus enhancing a drying process. The second is the formation of fine droplets at the sample and air interface that can be swept away by an air stream flowing above the sample surface, leading to a direct removal of moisture from the product. The formation is droplets or mist at product surface can be explained by the capillary wave theories [40], which related the misting effect to the unstable wave oscillations at the liquid-vapor interface [41]. According to Kudo et al. [41] the mist formation is influenced by factors such as the power and frequency of the applied US. Since the mist formation is a phase-change free water removal process that occurs in the initial stage of CUD, it should be a major contributor to the rapid drying in the initial stages of albumen drying.

3.1.1. Effective moisture diffusivity and activation energy

A food matrix binds water molecules to solid through various chemical bonds. Drying is a diffusion-controlled process, better understood through moisture diffusivities. Fig. 2e and f show that ultrasound application increases the effective diffusivities of water molecules in albumen, with higher ultrasound amplitudes further enhancing diffusivities. The average effective moisture diffusivities ($D_{eff,avg}$) in Table S2 increased by 114 % when the temperature rose from 40 °C to 60 °C. CUD40A40 and CUD40A60 amplitude increased $D_{eff,avg}$ by 119 % and 247 %. The effect of US diminished with higher temperatures, showing a 32 % and 91 % increase for CUD60A40 and CUD60A60, respectively. Magalhães et al. [42] reported similar findings for US-assisted apple drying. The increase in $D_{eff,avg}$ was due to higher mass transfer rates at a higher temperature and ultrasound-induced mist formation. The E_a values required for removing one mole of water during drying [17] are shown in Table S3, which were 32.929, 11.085, and 7.048 kJ/mol for HAD, CUD at 40 %, and CUD at 60 % amplitude, respectively. The lower E_a in the CUD process indicated less energy was needed for moisture removal, consistent with the findings of Rashid et al. [17] on sweet potato drying with ultrasound.

3.2. Albumen quality and functional attributes

3.2.1. Color parameters

One major parameter influencing consumer preferences is the color of the product, which determines its sensorial property. Any quality

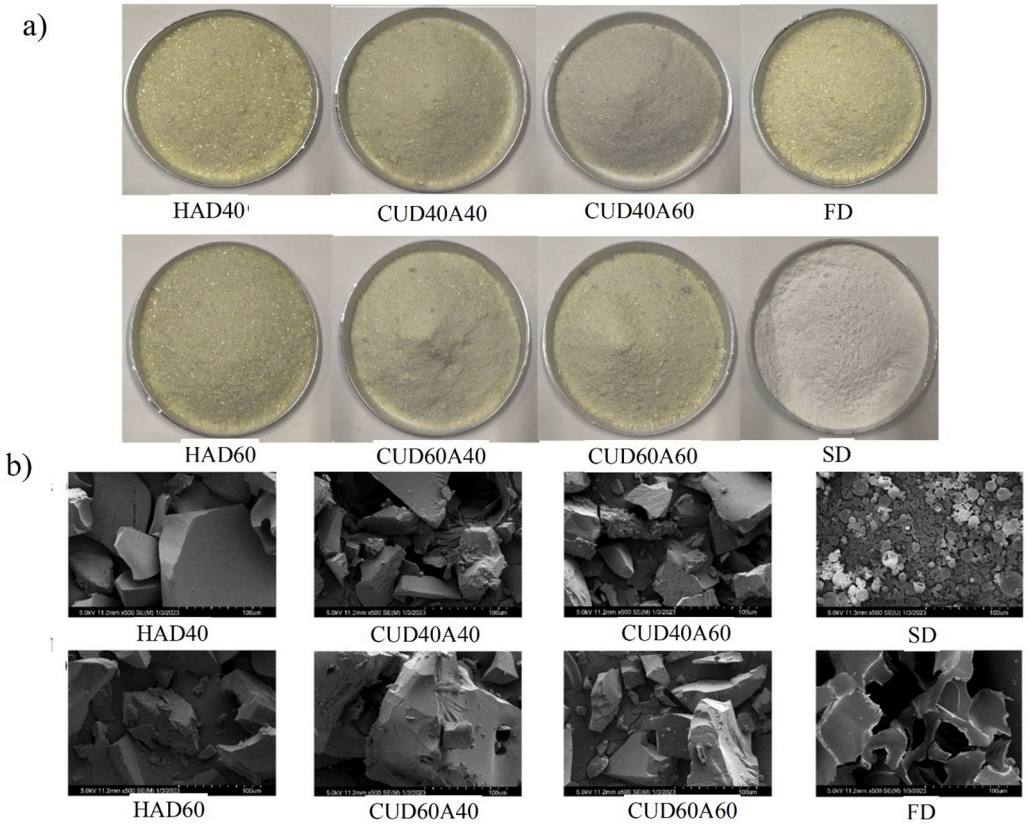

Fig. 3. a) Image and b) morphology of dried egg white (EW) powders.
HAD40 = Hot Air Drying (HAD) at 40 °C, HAD60 = HAD at 60 °C; CUD40A40 = Contact Ultrasound Drying (CUD) at 40 °C and 40 % amplitude, CUD60A40 = CUD at 60 °C and 40 % amplitude, CUD40A60 = CUD at 40 °C and 60 % amplitude, CUD60A60 = CUD at 60 °C and 60 % amplitude., FD = Freeze Drying, SD = Spray Drying.

issues with raw materials can affect the final product's color [43]. The images of dried EW powders are shown in the Fig. 3a. The color values of albumen powders are reported in Table 2, using the $L^*a^*b^*$ color scale, where L^* indicates brightness with a higher L^* value indicating a whiter product. The HAD40 and HAD60 samples had the lowest L^* values, likely due to an extended exposure of protein to high temperatures. In contrast, the CUD-dried albumen at both temperatures had significantly higher L^* values than HAD ($p < 0.05$), indicating less heat damage and discoloration due to shorter drying times. At a higher US amplitude, e.g. CUD60A60, a further increased L^* values at both temperatures can be observed. The FD and SD processes achieved the highest L^* values (91.55 and 94.48, respectively). The short residence times of the SD process and the low-temperature moisture removal of the FD process prevented heat damage and discoloration. Islam et al. [44] also reported lower L^* values with increased ultrasound power during the drying of vegetable soybean. Most samples exhibited similar yellowness (+b^*), except for the SD process, which had the lowest b^* value of 6.48.

The BI is crucial for determining the quality of the final albumen product and understanding the effects of the drying process. The HAD samples had the highest BI due to prolonged heat exposure. In contrast, the CUD sample had significantly lowered BI values in albumen powders at both temperature levels. At US amplitude of 60 % in CUD, a further reduced the BI compared to that at 40 % amplitude can be observed, indicating the importance of amplitude in controlling browning. The BI of FD samples was higher than the US treated but there is no significant difference between them. Overall, the drying process significantly impacts the color and the final quality of albumen powders. CUD yielded relatively low browning, partially due to shorted drying time a thus less exposure to elevated temperatures. Similarly, Tayyab Rashid [45] found that US-assisted convective drying of sweet potatoes resulted in lower BI values, slowing the formation of brown pigments.

3.2.2. Densities, flow indices, and water activity

For powdered products like albumen, physical properties such as bulk and tapped densities and flow characteristics are crucial for transportation and storage [46]. These properties, reported in Table 3, were assessed using the CI and HR. HAD samples showed the highest bulk (0.619 g/mL) and tapped densities (0.668 g/mL). All drying methods, except SD, showed no significant difference in flow indices (CI and HR) and had excellent flow characteristics. In addition, there were no significant differences in density between air dried albumen powders and CUD samples, though a high amplitude levels (60 %) in albumen powders resulted in slightly lower bulk densities. The lower densities in CUD samples compared to HAD may be due to a porous structure formed during drying, due to vibrational moisture removal. The FD- and SD-dried albumen had significantly lower density values due to their respective drying processes that maintain structural integrity and introduce pores [47]. Similar effects were noted for drying of plant protein [48] and mango powder [49].

The a_w is critical for shelf life and stability, and all dried samples had a_w of below 0.4 (Table 3). The US process achieved significantly lower a_w values compared to HAD, which provides benefits in enhancing microbial safety and reducing chemical and enzymatic degradation risks [47]. Thus, the drying method significantly impacts the final product's particle properties.

3.2.3. SEM

SEM offers high-resolution microscopic images, allowing the study of surface and particle morphology with a small sample. The SEM images of the albumen powders are shown in Fig. 3b.

In the HAD-albumen samples, the particles exhibited smooth surfaces, sharp and uneven edges, and small sheets-like patterns. Since the albumen was applied to drying surface in a thin layer during HAD, the removal of moisture left behind a thin and flat sold sheet, resulting in the morphology observed in Fig. 3b. In contrast, the surface of the CUD-albumen showed small pores on the smooth surface. These pores likely form due to the microcapillary action of acoustic cavitation. Their presence may enhance the functional properties of CUD-albumen, such as solubility, due to enhanced hydration. Similar results were reported by Du et al. [50] who noticed microstructural changes due to the application of US on dried pumpkin seed proteins. The FD-albumen samples exhibited a porous network likely formed due to moisture removal through sublimation under vacuum, with no or minimal volume collapse. On the other hand, small spherical particles can be observed in the SD-albumen samples. In addition, the surface of the SD-albumen particles had a wrinkled surface with vacuoles in the surface. Preethi et al. [47] also reported similar observations in their SD-albumen powders. The wrinkled surface of the SD-albumen powders could be a result of the rapid water removal with an accompanied shrinkage on the particle surface [50]. Therefore, different drying methods give rise to different microstructural and surface morphologies.

3.2.4. CD spectroscopy

Circular dichroism (CD) spectroscopy is a valuable tool for examining the secondary conformations of proteins, based on the differential absorption of circularly polarized light. CD signals were recorded in the wavelength range of 190–260 nm [51], as shown in Fig. 4a, and revealed that different drying methods significantly influence protein conformation. The secondary structure of proteins, which includes α-helices, β-sheets, β-turns, and random coils, is critical for maintaining protein integrity, primarily due to the stabilizing hydrogen bonds within α-helices and β-sheets.

The application of ultrasound during contact ultrasonic drying (CUD) notably altered the secondary structure of albumen proteins. In the samples treated with ultrasound, there was a marked reduction in α-helix and β-sheet content, alongside an increase in β-turns and random coils. This structural change is likely due to the effects of acoustic cavitation, which generates localized high mechanical stress zones that disrupt hydrogen bonds, leading to the unfolding of proteins and alterations in their secondary structure. The extent of this disruption was greater in samples dried at 40 % ultrasound amplitude, which required a longer drying time compared to those dried at 60 %, resulting in a more

Table 2
Color parameters and browning index of egg white powders dried using different techniques.

Sample code*	L^*	a^*	b^*	Browning Index (BI)
HAD40	81.05 ± 2.6^{cd}	-2.87 ± 0.1^{b}	20.74 ± 2.26^{a}	26.12 ± 3.31^{a}
HAD60	79.86 ± 1.15^{d}	-3.15 ± 0.15^{bc}	18.78 ± 0.98^{a}	23.10 ± 1.19^{ab}
CUD40A40	82.22 ± 1.65^{bc}	-3.35 ± 0.23^{cd}	19.98 ± 1.75^{a}	22.99 ± 1.81^{ab}
CUD60A40	82.42 ± 0.17^{bc}	-3.50 ± 0.38^{d}	18.26 ± 2.59^{a}	21.19 ± 3.98^{b}
CUD40A60	82.80 ± 0.57^{bc}	-3.08 ± 0.19^{bc}	15.01 ± 1.03^{b}	16.69 ± 1.31^{c}
CUD60A60	83.51 ± 0.74^{b}	-3.57 ± 0.17^{d}	18.59 ± 1.15^{a}	20.86 ± 1.08^{b}
SD	94.49 ± 0.06^{a}	-1.17 ± 0.03^{a}	6.48 ± 0.06^{c}	6.02 ± 0.05^{d}
FD	91.55 ± 0.07^{a}	-1.58 ± 0.02^{a}	21.61 ± 0.29^{a}	24.95 ± 0.39^{ab}

* HAD40 = Hot Air Drying (HAD) at 40 °C, HAD60 = HAD at 60 °C; CUD40A40 = Contact Ultrasound Drying (CUD) at 40 °C and 40 % amplitude, CUD60A40 = CUD at 60 °C and 40 % amplitude, CUD40A60 = CUD at 40 °C and 60 % amplitude, CUD60A60 = CUD at 60 °C and 60 % amplitude., FD = Freeze Drying, SD = Spray Drying. For each column different small letters denote a significant difference ($p < 0.05$).

Table 3
Density parameters, flow indices, flowability and water activity (aw) of egg white powders dried using different techniques.

Sample code*	Bulk density (g/cm^3)	Tapped density (g/cm^3)	Hausner ratio (HR)	Carr index (CI)	Flow characteristic	a_w
HAD40	0.619 ± 0.015^{a}	0.668 ± 0.011^{a}	1.079 ± 0.013^{b}	7.333 ± 1.154^{b}	Excellent	0.396 ± 0.006^{a}
HAD60	0.612 ± 0.003^{ab}	0.650 ± 0.001^{ab}	1.056 ± 0.012^{b}	5.333 ± 1.154^{b}	Excellent	0.367 ± 0.002^{b}
CUD40A40	0.595 ± 0.012^{ab}	0.649 ± 0.020^{ab}	1.079 ± 0.013^{b}	7.333 ± 1.154^{b}	Excellent	0.241 ± 0.001^{c}
CUD60A40	0.5940 ± 0.013^{ab}	0.650 ± 0.006^{ab}	1.095 ± 0.013^{b}	8.666 ± 1.154^{b}	Excellent	0.223 ± 0.001^{d}
CUD40A60	0.588 ± 0.005^{b}	0.630 ± 0.003^{b}	1.071 ± 0.013^{b}	6.666 ± 1.154^{b}	Excellent	0.195 ± 0.001^{e}
CUD60A60	0.593 ± 0.001^{ab}	0.636 ± 0.009^{ab}	1.071 ± 0.013^{b}	6.666 ± 1.154^{b}	Excellent	0.174 ± 0.002^{f}
SD	0.253 ± 0.0^{d}	0.346 ± 0.016^{c}	1.377 ± 0.044^{a}	27.333 ± 2.309^{a}	Poor	0.174 ± 0.003^{f}
FD	0.285 ± 0.011^{c}	0.308 ± 0.014^{d}	1.079 ± 0.006^{b}	7.333 ± 0.577^{b}	Excellent	0.157 ± 0.004^{g}

* HAD40 = Hot Air Drying (HAD) at 40 °C, HAD60 = HAD at 60 °C; CUD40A40 = Contact Ultrasound Drying (CUD) at 40 °C and 40 % amplitude, CUD60A40 = CUD at 60 °C and 40 % amplitude, CUD40A60 = CUD at 40 °C and 60 % amplitude, CUD60A60 = CUD at 60 °C and 60 % amplitude., FD = Freeze Drying, SD = Spray Drying. For each column different small letters denote a significant difference ($p < 0.05$).

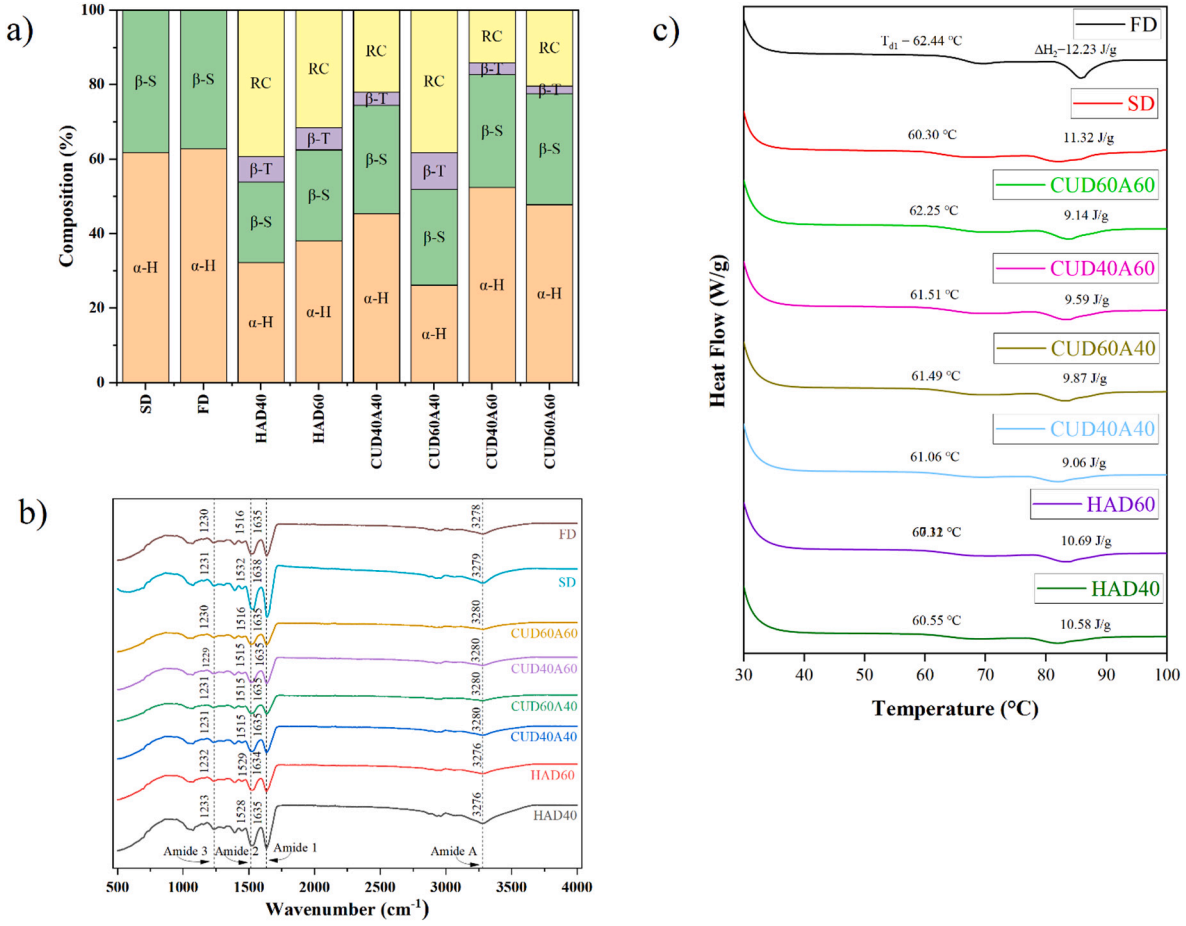

Fig. 4. a) Secondary structure proportion (%) (α-H: α-helix, β-S: β-sheet, β-T: β-turn, and RC: random coil forms), b) FTIR spectra, and c) thermal behaviour of egg whites (EW) dried using different drying techniques.
HAD40 = Hot Air Drying (HAD) at 40 °C, HAD60 = HAD at 60 °C; CUD40A40 = Contact Ultrasound Drying (CUD) at 40 °C and 40 % amplitude, CUD60A40 = CUD at 60 °C and 40 % amplitude, CUD40A60 = CUD at 40 °C and 60 % amplitude, CUD60A60 = CUD at 60 °C and 60 % amplitude., FD = Freeze Drying, SD = Spray Drying.

pronounced formation of random coils and β-turns (Fig. 4a- S1).

These findings are consistent with previous research on ultrasonically assisted spray drying of egg whites, which also reported increased random coil and β-turn content due to sonication-induced structural changes [51]. In contrast, no significant alterations in the secondary structure were observed in freeze-dried (FD) and spray-dried (SD) albumen powders, as reflected in their CD spectra (Fig. 4a-S1). The absence of random coil and β-turn structures in these samples can be attributed to the denaturation of proteins, such as ovalbumin, during the drying process. Spray drying exposes proteins to high temperatures, while freeze drying involves ice crystallization, both of which lead to protein denaturation. In these conditions, denatured proteins tend to aggregate into more ordered β-sheet and α-helix structures through protein-protein interactions [52]. The loss of water further drives this shift from flexible random coil and β-turn configurations to more rigid structures, explaining their absence in FD and SD samples [52]. Wang et al. [53] and Cobb et al. [54] reported similar structural transitions where heat treatment led to a decrease in random coil and β-turn content due to unfolding and subsequent aggregation. Moreover, Lee et al. [55] and Perlitz et al. [56] emphasized the role of dehydration in this shift, highlighting that both heat and moisture removal induce a transition from flexible regions to stable, ordered structures.

The results from CD spectroscopy clearly demonstrate that CUD induces significant changes in the secondary structure of proteins, causing greater unfolding and disarray compared to conventional drying methods.

3.2.5. Fourier-transform infrared spectroscopy (FTIR)

FTIR was used to investigate protein secondary structure and conformational changes induced by drying, which detected vibrations in the Amide A (3200–3500 cm^{-1}), Amide *I* (1600–1700 cm^{-1}), Amide II (1480–1580 cm^{-1}), and Amide III (1200–1400 cm^{-1}) regions [57]. The obtained FTIR spectra are presented in Fig. 4b. The albumen powders possess various bonds that interact with the infrared region of the spectra, enabling observation of changes in the secondary structure. The Amide A region represents the N—H bond vibrations that can be seen in all of the samples studied. A small peak shift to a higher wavenumber can be discerned in CUD-albumen (3280 cm^{-1}) compared to HAD-albumen (3276 cm^{-1}). The disruption of hydrogen bonding led to this change observed in the CD spectra. Breaking these bonds exposed more hydrophilic functional groups, helping to improve the functional attributes of CUD-albumen samples. The Amide I region has various peaks corresponding to the secondary structure of β-sheet (1610–1642 cm^{-1}), α-helix (1650–1659 cm^{-1}), and random coil (1643–1650 cm^{-1}) [57]. In the Amide II region, the peaks of CUD-albumen and FD-albumen shifted to 1516 cm^{-1}, compared to that of HAD-albumen at 1529 cm^{-1}. The Amide II region also relates to the α-helix and β-sheet structures. The change in wavenumber indicates a change in protein secondary structure. FTIR analysis showed a blue shift in the Amide II region peak to 1516 cm^{-1} for CUD and FD samples, compared to 1529 cm^{-1} for HAD. This shift indicates an alteration in protein secondary structure. On the other hand, SD-albumen showed an increase in the Amide 2 region peak to 1532 cm^{-1}. All samples displayed an Amide III peak between 1230 and 1233 cm^{-1}. These results confirm that CUD induces structural changes more effectively than other drying methods.

3.2.6. Differential scanning calorimetry (DSC)

Changes in denaturation properties of proteins directly affect their gel formation and functional properties. Alterations in protein secondary structure result in energy absorption, known as denaturation enthalpy [58]. According to the literature, the thermograms of albumen have two endothermic peaks [58,59]. The first peak corresponds to the denaturation enthalpy (ΔH_1) of ovotransferrin and lysozyme, occurring in the range of 60–72 °C. The second peak (ΔH_2) corresponds to the unfolding of ovalbumin, occurring around 80–85 °C.

From the thermograms of albumen determined by DSC, we determined the denaturation enthalpies (ΔH) and the denaturation temperatures (T_d) of the albumen powders, as shown in Fig. 4c and Table S4. Similar to the reports of others [58,59], we also observed 2 peaks. The FD-albumen powders exhibited the lowest enthalpies (ΔH_1 = 3.4 J/g) for the ovotransferrin peak, while the HAD-albumen samples had relatively high denaturation enthalpies, e.g., 5.694 J/g and 6.513 J/g for HAD40 and HAD60, respectively. The application of ultrasound significantly lowered the enthalpies at both temperatures and amplitudes. For CUD40A40 and CUD40A60, the enthalpies significantly lowered by ~33 %. At 60 °C, the enthalpies decreased by 21 % and 26 % for CUD60A40 and CUD60A60, respectively. The ovalbumin peak (ΔH_2) followed a similar trend, where the application of ultrasound lowered denaturation enthalpies.

The CUD-albumen samples had higher denaturation temperatures (T_{d1}) of ovotransferrin than the hot air dried. The FD recorded the highest first peak (62.44 °C), whereas the SD sample had the lowest T_{d1}. This is in agreement with the report of Ma et al. [60]. Changes in protein structure, resulting in partial denaturation and unfolding, become evident from the thermal properties. The CUD process promotes exposure of the material to high mechanical forces from acoustic cavitation, which could lead to protein unfolding and intramolecular bond disruption. This could lower energy required for unfolding of US-treated albumen, exposing other functional groups to environment and enhancing its functional properties [57]. The lowered ΔH indicates that these changes in albumen protein reduced the energy required for denaturing the protein. Özdemir et al. [61] reported a similar trend where the application of ultrasound to whey proteins lowered the denaturation enthalpies. They suggested that sonication caused proteins to adopt a more open state while also favoring ionic and hydrophobic interactions within the protein. A similar study on black bean protein isolates by Li et al. [62] also showed that the application of US at low (150 W) and medium power (300 W) lowered the denaturation enthalpies and temperatures, with longer exposure times causing more reductions.

3.2.7. Free sulphydryl, total sulphydryl, and disulfide content

The reactivity of sulphydryl and disulfide linkages plays a significant role in the functional properties of albumen, such as foaming and gelling [63]. Albumen contains a number of proteins, among which ovalbumin is the only one with free sulphydryl groups [64]. The total sulphydryl, free sulphydryl, and disulfide content of the albumen are shown in Fig. 5a.

The HAD at 40 °C (0.90 μmoles/g) followed by SD (1.01 μmoles/g) and HAD60 samples (1.03 μmoles/g) had the lowest amount of free sulphydryl content. The could be attributed to the heat degradation and partial denaturation of the proteins. The FD-albumen sample, as expected, showed significantly high free-SH content (1.38 μmoles/g), due to the absence of heat treatment. The application of ultrasound significantly improved the free -SH content. At 40 % amplitude, there was a 57 % and 21 % increase at 40 °C and 60 °C, respectively. Similar increases in the free -SH content can be observed at the amplitude of 60 %. Chen et al. [32] also reported similar results on egg white proteins. The unfolding and structural changes due to sonication must have led to the exposure of more of the -SH groups. This unfolding and the changes in secondary structure can also be seen in the CD spectroscopy (Fig. 4a). Also, the capillary action and mechanical vibrations can result in more surface area to be exposed and the formation of finer particles, leading to increased free sulphydryl content. With respect to the total sulphydryl content, all samples except for the FD (2.13 μmoles/g) did not have significant differences among themselves. An inverse relation could be established between the contents of the S—S links and the free-SH links. All the CUD samples showed significantly lower S—S link content. The decrease in the S—S linkage could be due to the rupture of these linkages as a consequence of the high shear from the cavitation phenomena. The dissociation of these linkages formed new free -SH linkages, thus also causing an increase in the total exposed -SH linkages [32]. The increased free-SH groups are crucial for improving various functional properties of the albumen, such as foaming. The application of ultrasonic waves significantly affects and increases the free sulphydryl content, demonstrating the impact of the drying process.

3.2.8. Foaming properties

The foaming capacities and stability of albumen powders are presented in Fig. 5b. The CUD samples demonstrated significantly higher foaming capacity and stability compared to all other samples across all drying conditions (temperature and amplitude). The enhanced foaming properties observed in CUD-albumen samples can be attributed to several factors: i) The increased solubility of the albumen powder resulting from CUD drying (refer to Fig. 5c) enhances the availability of proteins in the aqueous phase, facilitating the formation of stable foam. For optimal foaming capacity, it is crucial that proteins can readily stabilize at the interface. ii) Sonication during CUD might induce capillary effects and create finer particles, thereby increasing the surface area of the samples. This expanded surface area allows more proteins and functional groups to be available for foaming, as supported by SEM images showing the refined particle structure (refer to Fig. 3b). iii) Structural changes in the proteins, as observed through CD spectra (refer to Fig. 4a), expose more hydrophilic groups. This change enhances the

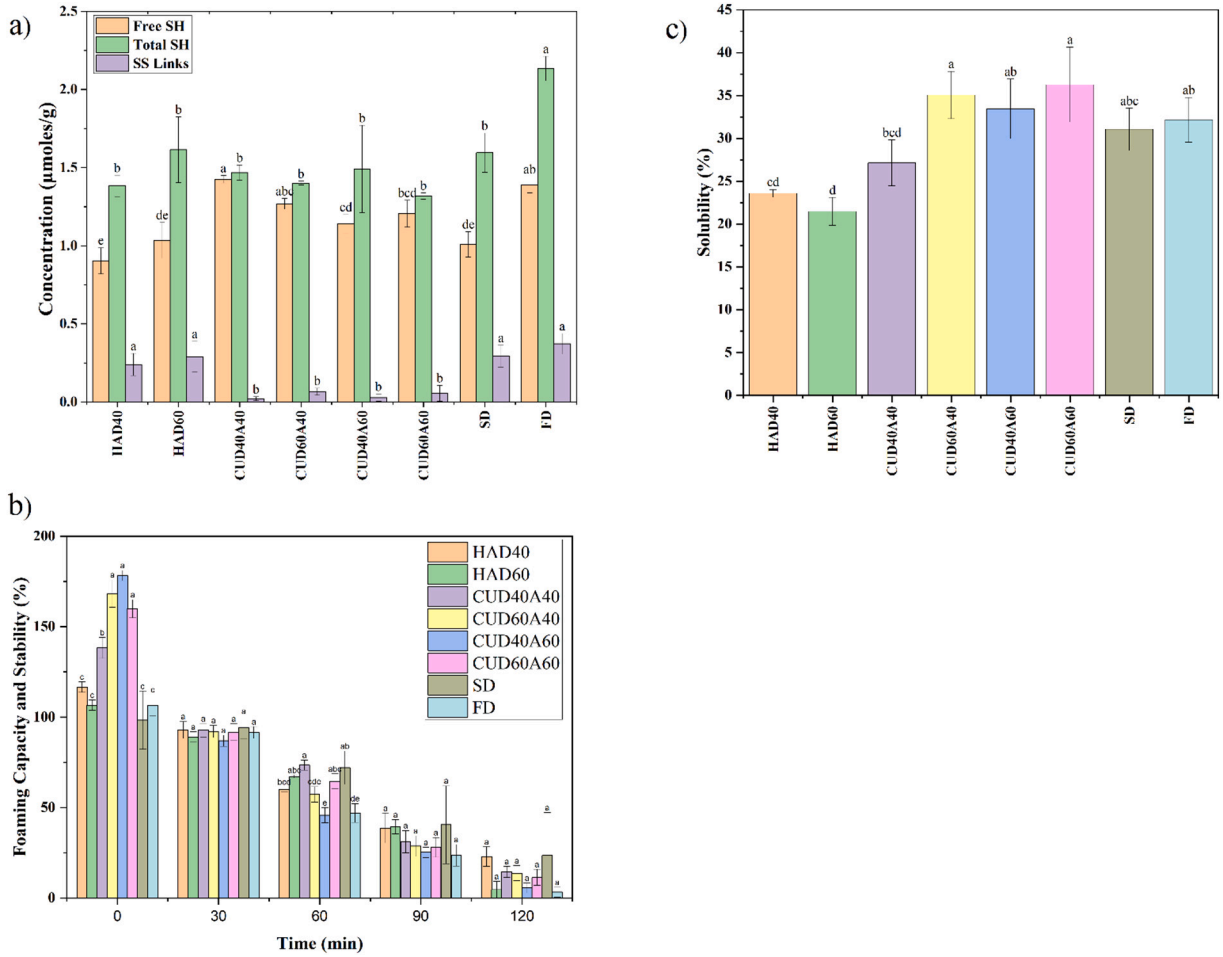

Fig. 5. a) Sulphydryl group content, b) foaming properties, and c) solubility (%) of egg whites dried using different drying techniques.
HAD40 = Hot Air Drying (HAD) at 40 °C, HAD60 = HAD at 60 °C; CUD40A40 = Contact Ultrasound Drying (CUD) at 40 °C and 40 % amplitude, CUD60A40 = CUD at 60 °C and 40 % amplitude, CUD40A60 = CUD at 40 °C and 60 % amplitude, CUD60A60 = CUD at 60 °C and 60 % amplitude, FD = Freeze Drying, SD = Spray Drying.

binding capacity at the air-water interface, crucial for forming and stabilizing foam. iv) Ultrasound application in the CUD process likely causes the dissociation of disulfide linkages, increasing the content of free sulphydryl groups. This alteration in the protein structure further aids in improving the foaming properties by enhancing protein flexibility and reactivity at the interface. These -SH groups are essential and directly linked to the foaming capacity, which explains the improved foaming in the CUD samples [65].

3.2.9. Soluble protein content

An important functional property of proteins is their solubility. Protein solubility can be defined as the ratio of protein in the aqueous phase to that total in both solid and aqueous phases [66]. The protein solubilities of different treatments are shown in Fig. 5c.

The HAD40 (23.57 %) and HAD60 (21.47 %) albumen samples had the lowest solubility of all the samples. This clearly results from the prolonged exposure of the samples to heat during HAD. The observed decrease in albumen solubility indicates partial denaturation of the proteins, due to the extensive heat exposure leading to structural changes. On the other hand, FD involves minimal heat exposure among all the drying methods, resulting in the FD samples having one of the highest solubilities (32.15 %). SD-albumen (31.25 %) also had a solubility higher than HAD samples. The application of ultrasound significantly improved the solubility (CUD60A60: 36.28 %, CUD60A40: 35.05 %, and CUD40A60: 33.43 %). The CUD at 60 °C reported the highest solubility (36.28 %) among all the samples. The micro-scale mechanical activities due to acoustic cavitation, e.g., high shear forces (micro streaming), shock waves, water jets, localized heat and pressure gradients may cause partial unfolding of the proteins. They may also allow more hydrophilic residues and functional groups to become available on the albumen surface for interaction with the aqueous phase, increasing solubility [57]. In addition, the ultrasonic waves may also alter the physical and structural properties during drying. The vibrations cause the particles to break, thereby increasing their total exposed surface area. A similar effect has also been reported by Jambrak et al. [67] who showed the US lowers the particle size and size distribution of whey protein isolates. The small pores on the surface of CUD samples, as seen on SEM images, might have also aided in hydration, thus enhancing the solubility. The changes in the secondary structures, as shown by the random coil and β-turn in the CD spectra of CUD, influence the overall flexibility and surface exposure of hydrophilic residues, which provides additional explanation for the increased solubility [51]. Thus, solubility is closely linked to the drying method, with CUD improving the solubility.

4. Conclusion

This study demonstrates the efficacy of contact ultrasonic drying (CUD) as a novel, sustainable method for drying albumen, offering significant advantages over traditional drying techniques such as hot air drying (HAD), spray drying (SD), and freeze drying (FD). CUD enhanced drying kinetics, evidenced by a reduction in drying times and activation

energy (Ea), while increasing the effective moisture diffusivity compared to HAD. The application of ultrasound during drying improved protein integrity by maintaining more native structures and reducing denaturation enthalpies. The significant reduction in browning index and enhanced color retention in CUD samples highlighted its potential for minimizing thermal degradation. Importantly, the solubility of the albumen powders was significantly improved in CUD-treated samples, particularly at higher ultrasound amplitudes. Solubility is a crucial functional property for protein powders, impacting their application in food systems. The enhanced solubility can be attributed to the alterations in microstructure and secondary protein structure. SEM images revealed that CUD-produced powders exhibited more porous and finer particle structures, increasing surface area and promoting better hydration. Additionally, CD spectroscopy indicated that CUD caused structural changes, with a higher proportion of random coil and β-turn structures compared to the more rigid, denatured forms (e.g., β-sheets and α-helices) found in HAD and SD samples. These structural changes facilitated improved water interaction, thereby enhancing solubility. The disruption of disulfide bonds and the exposure of free sulfhydryl groups in CUD samples also contributed to the improved functional properties, including foaming capacity and stability. These findings underscore the ability of CUD to not only enhance the drying efficiency but also preserve and improve the functional qualities of the resulting protein powders.

Overall, CUD emerges as a promising alternative to conventional drying methods, offering improved protein functionality, better solubility, and reduced processing time. Future research should focus on exploring the impact of CUD on protein digestibility, long-term shelf stability, and microbial safety, ensuring the broad applicability of this green technology for high-protein food materials.

Abbreviations

BD	bulk density
BI	browning index
CD	circular dichroism spectroscopy
CI	Carr's compressibility index
CUD	contact ultrasonic drying
FC	foaming capacity
FS	foaming stability
HAD	hot air drying
HR	Hausner ratio
FD	freeze drying
RSS	residual sum of squares
SD	spray drying
SEM	scanning electron microscopy
TD	tapped density
US	ultrasound

CRediT authorship contribution statement

Vedant Mundada: Writing – original draft, Methodology, Investigation, Formal analysis, Data curation. **Gulsah Karabulut:** Writing – review & editing, Methodology, Investigation, Formal analysis, Data curation. **Ragya Kapoor:** Investigation. **Amir Malvandi:** Investigation. **Hao Feng:** Writing – review & editing, Supervision, Project administration, Methodology, Funding acquisition, Conceptualization.

Funding sources

This work was supported by the National Science Foundation (NSF) Grant #IIP 16-24812 I/UCRC IA.

Declaration of competing interest

The authors declare that they have no known competing financial interests or personal relationships that could have appeared to influence the work reported in this paper.

Acknowledgements

The authors would like to thank the scientists at the Materials Research Laboratory Central Research Facilities at University of Illinois for their assistance with the Scanning Electron Microscopy. The authors also acknowledge Mark Gnaedinger for his assistance with the operation of the ultrasonic contact dryer and Dr. Youngsoo Lee for his assistance with spray drying.

Appendix A. Supplementary data

Supplementary data to this article can be found online at https://doi.org/10.1016/j.ijbiomac.2024.137664.

Data availability

Data will be made available on request.

References

[1] J. Wu, Eggs and egg products processing, in: Food Processing, John Wiley & Sons, Ltd, Chichester, UK, 2014, pp. 437–455, https://doi.org/10.1002/9781118846315.ch19.
[2] M.F. Medina-Cruz, D. Zárate-Contreras, R.V. Pérez-Ruiz, J.E. Aguilar-Toalá, M. Rosas-Espejel, R.G. Cruz-Monterrosa, Nutritional aspects, production and viability in the market of organic chicken eggs: review, Food Chem. Adv. 4 (2024), https://doi.org/10.1016/j.focha.2023.100595.
[3] S.M. Razi, H. Fahim, S. Amirabadi, A. Rashidinejad, An overview of the functional properties of egg white proteins and their application in the food industry, Food Hydrocoll. 135 (2023), https://doi.org/10.1016/j.foodhyd.2022.108183.
[4] R. Agregán, P.E.S. Munekata, P. Putnik, M. Pateiro, D. Bursać Kovačević, S. Zavadlav, J.M. Lorenzo, The use of novel technologies in egg processing, Food Rev. Intl. (2021) 1–21, https://doi.org/10.1080/87559129.2021.1980887.
[5] J. Zang, M. Qing, Y. Ma, Y. Chi, Y. Chi, Shelf-life modeling for whole egg powder: application of the general stability index and multivariate accelerated shelf-life test, J. Food Eng. 340 (2023), https://doi.org/10.1016/j.jfoodeng.2022.111313.
[6] W. Katekhong, S. Charoenrein, Color and gelling properties of dried egg white: effect of drying methods and storage conditions, Int. J. Food Prop. 20 (2017) 2157–2168, https://doi.org/10.1080/10942912.2016.1233429.
[7] Y. Shen, X. Tang, Y. Li, Drying methods affect physicochemical and functional properties of quinoa protein isolate, Food Chem. 339 (2021) 127823, https://doi.org/10.1016/j.foodchem.2020.127823.
[8] S. Renzetti, I.A.F. van den Hoek, R.G.M. van der Sman, Amino acids, polyols and soluble fibres as sugar replacers in bakery applications: egg white proteins denaturation controlled by hydrogen bond density of solutions, Food Hydrocoll. 108 (2020), https://doi.org/10.1016/j.foodhyd.2020.106034.
[9] R. Kapoor, G. Karabulut, V. Mundada, H. Feng, Unraveling the potential of non-thermal ultrasonic contact drying for enhanced functional and structural attributes of pea protein isolates: a comparative study with spray and freeze-drying methods, Food Chem. 439 (2024), https://doi.org/10.1016/j.foodchem.2023.138137.
[10] J.A. Moses, T. Norton, K. Alagusundaram, B.K. Tiwari, Novel drying techniques for the food industry, Food Eng. Rev. 6 (2014) 43–55, https://doi.org/10.1007/s12393-014-9078-7.
[11] N. Gharbi, M. Labbafi, Effect of processing on aggregation mechanism of egg white proteins, Food Chem. 252 (2018) 126–133, https://doi.org/10.1016/j.foodchem.2018.01.088.
[12] D. Huang, K. Men, D. Li, T. Wen, Z. Gong, B. Sunden, Z. Wu, Application of ultrasound technology in the drying of food products, Ultrason. Sonochem. 63 (2020) 104950, https://doi.org/10.1016/j.ultsonch.2019.104950.
[13] G. Yildiz, J. Ding, J. Andrade, N.J. Engeseth, H. Feng, Effect of plant protein-polysaccharide complexes produced by mano-thermo-sonication and pH-shifting on the structure and stability of oil-in-water emulsions, Innov. Food Sci. Emerg. Technol. 47 (2018) 317–325, https://doi.org/10.1016/j.ifset.2018.03.005.
[14] H. Lee, B. Zhou, H. Feng, S.E. Martin, Effect of pH on inactivation of escherichia coli K12 by sonication, manosonication, thermosonication, and manothermosonication, J. Food Sci. 74 (2009), https://doi.org/10.1111/j.1750-3841.2009.01130.x.
[15] G. Karabulut, S. Yildiz, A.C. Karaca, O. Yemiş, Ultrasound and enzyme-pretreated extraction for the valorization of pea pod proteins, J. Food Process Eng. (2023), https://doi.org/10.1111/jfpe.14452.
[16] L.A. Scripcă, S. Amariei, The use of ultrasound for preventing honey crystallization, Foods 10 (2021) 773, https://doi.org/10.3390/foods10040773.
[17] A. Malvandi, D. Nicole Coleman, J.J. Loor, H. Feng, A novel sub-pilot-scale direct-contact ultrasonic dehydration technology for sustainable production of distillers dried grains (DDG), Ultrason. Sonochem. 85 (2022) 105982, https://doi.org/10.1016/j.ultsonch.2022.105982.

[18] R. Kapoor, G. Karabulut, V. Mundada, H. Feng, Non-thermal ultrasonic contact drying of pea protein isolate suspensions: effects on physicochemical and functional properties, Int. J. Biol. Macromol. 253 (2023) 126816, https://doi.org/10.1016/j.ijbiomac.2023.126816.
[19] O. Kahraman, A. Malvandi, L. Vargas, H. Feng, Drying characteristics and quality attributes of apple slices dried by a non-thermal ultrasonic contact drying method, Ultrason. Sonochem. 73 (2021) 105510, https://doi.org/10.1016/j.ultsonch.2021.105510.
[20] H. Naidu, O. Kahraman, H. Feng, Novel applications of ultrasonic atomization in the manufacturing of fine chemicals, pharmaceuticals, and medical devices, Ultrason. Sonochem. 86 (2022), https://doi.org/10.1016/j.ultsonch.2022.105984.
[21] A. Malvandi, D. Nicole Coleman, J.J. Loor, H. Feng, A novel sub-pilot-scale direct-contact ultrasonic dehydration technology for sustainable production of distillers dried grains (DDG), Ultrason. Sonochem. 85 (2022), https://doi.org/10.1016/j.ultsonch.2022.105982.
[22] J. Cai, R. Lopez, Y. Lee, Effect of feed material properties on microencapsulation by spray drying with a three-fluid nozzle: soybean oil encapsulated in maltodextrin and sugar beet pectin, J. Food Process. Preserv. 2023 (2023) 4974631, https://doi.org/10.1155/2023/4974631.
[23] W. Katekhong, S. Charoenrein, Influence of spray drying temperatures and storage conditions on physical and functional properties of dried egg white, Drying Technol. 36 (2018) 169–177, https://doi.org/10.1080/07373937.2017.1307218.
[24] J.J. Moré, The Levenberg-Marquardt Algorithm: Implementation and Theory, in, 1978, pp. 105–116, https://doi.org/10.1007/BFb0067700.
[25] J. Crank, The Mathematics of Diffusion, Oxford university press, 1979.
[26] A.R. Celma, F. Cuadros, F. López-Rodríguez, Convective drying characteristics of sludge from treatment plants in tomato processing industries, Food Bioprod. Process. 90 (2012) 224–234, https://doi.org/10.1016/j.fbp.2011.04.003.
[27] L.M. Bal, A. Kar, S. Satya, S.N. Naik, Kinetics of colour change of bamboo shoot slices during microwave drying, Int. J. Food Sci. Technol. 46 (2011) 827–833, https://doi.org/10.1111/j.1365-2621.2011.02553.x.
[28] R. Kapoor, H. Feng, Characterization of physicochemical, packing and microstructural properties of beet, blueberry, carrot and cranberry powders: the effect of drying methods, Powder Technol. 395 (2022) 290–300, https://doi.org/10.1016/j.powtec.2021.09.058.
[29] S.A. Malomo, R. He, R.E. Aluko, Structural and functional properties of hemp seed protein products, J. Food Sci. 79 (2014) C1512–C1521, https://doi.org/10.1111/1750-3841.12537.
[30] T.G. Kudre, S.K. Bejjanki, B.W. Kanwate, P.Z. Sakhare, Comparative study on physicochemical and functional properties of egg powders from Japanese quail and white Leghorn chicken, Int. J. Food Prop. 21 (2018) 957–972, https://doi.org/10.1080/10942912.2018.1466320.
[31] M.M. Bradford, A rapid and sensitive method for the quantitation of microgram quantities of protein utilizing the principle of protein-dye binding, Anal. Biochem. 72 (1976) 248–254, https://doi.org/10.1016/0003-2697(76)90527-3.
[32] Y. Chen, L. Sheng, M. Gouda, M. Ma, Impact of ultrasound treatment on the foaming and physicochemical properties of egg white during cold storage, LWT 113 (2019) 108303, https://doi.org/10.1016/j.lwt.2019.108303.
[33] Y. Lan, J.-B. Ohm, B. Chen, J. Rao, Physicochemical properties and aroma profiles of flaxseed proteins extracted from whole flaxseed and flaxseed meal, Food Hydrocoll. 104 (2020) 105731, https://doi.org/10.1016/j.foodhyd.2020.105731.
[34] G. Çalışkan Koç, B. Çabuk, FARKLI MİKRODALGA GÜÇLERİNİN KÖPÜK KURUTMA YÖNTEMİ İLE KURUTULMUŞ YUMURTA BEYAZI TOZLARININ KURUMA KİNETİĞİ VE TOZ ÜRÜN ÖZELLİKLERİ ÜZERİNE ETKİSİ, GIDA/THE JOURNAL OF FOOD 44 (2019) 328–339, https://doi.org/10.15237/gida.GD18126.
[35] D.I. Onwude, N. Hashim, R.B. Janius, N.M. Nawi, K. Abdan, Modeling the thin-layer drying of fruits and vegetables: a review, Compr. Rev. Food Sci. Food Saf. 15 (2016) 599–618, https://doi.org/10.1111/1541-4337.12196.
[36] W. Francis, M.C. Peters, Mass transfer in distillation and drying, in: Fuels and Fuel Technology, Elsevier, 1980, pp. 701–708, https://doi.org/10.1016/B978-0-08-025249-0.50117-8.
[37] P.C. Panchariya, D. Popovic, A.L. Sharma, Thin-layer modelling of black tea drying process, J. Food Eng. 52 (2002) 349–357, https://doi.org/10.1016/S0260-8774(01)00126-1.
[38] S.J. Babalis, V.G. Belessiotis, Influence of the drying conditions on the drying constants and moisture diffusivity during the thin-layer drying of figs, J. Food Eng. 65 (2004) 449–458, https://doi.org/10.1016/j.jfoodeng.2004.02.005.
[39] J.A. Gallego-Juárez, E. Riera, S. de la Fuente Blanco, G. Rodríguez-Corral, V. M. Acosta-Aparicio, A. Blanco, Application of high-power ultrasound for dehydration of vegetables: processes and devices, Drying Technol. 25 (2007) 1893–1901, https://doi.org/10.1080/07373930701677371.
[40] H. Feng, G. Barbosa-Canovas, J. Weiss (Eds.), Ultrasound Technologies for Food and Bioprocessing, Springer New York, New York, NY, 2011, https://doi.org/10.1007/978-1-4419-7472-3.
[41] T. Kudo, K. Sekiguchi, K. Sankoda, N. Namiki, S. Nii, Effect of ultrasonic frequency on size distributions of nanosized mist generated by ultrasonic atomization, Ultrason. Sonochem. 37 (2017) 16–22, https://doi.org/10.1016/j.ultsonch.2016.12.019.
[42] M.L. Magalhães, S.J.M. Cartaxo, M.I. Gallão, J.V. García-Pérez, J.A. Cárcel, S. Rodrigues, F.A.N. Fernandes, Drying intensification combining ultrasound pre-treatment and ultrasound-assisted air drying, J. Food Eng. 215 (2017) 72–77, https://doi.org/10.1016/j.jfoodeng.2017.07.027.
[43] R. Kapoor, H. Feng, Characterization of physicochemical, packing and microstructural properties of beet, blueberry, carrot and cranberry powders: the effect of drying methods, Powder Technol. 395 (2022) 290–300, https://doi.org/10.1016/j.powtec.2021.09.058.
[44] M. Islam, M. Zhang, D. Fan, Ultrasonically enhanced low-temperature microwave-assisted vacuum frying of edamame: effects on dehydration kinetics and improved quality attributes, Drying Technol. 37 (2019) 2087–2104, https://doi.org/10.1080/07373937.2018.1558234.
[45] M. Tayyab Rashid, K. Liu, M. Ahmed Jatoi, B. Safdar, D. Lv, D. Wei, Developing ultrasound-assisted hot-air and infrared drying technology for sweet potatoes, Ultrason. Sonochem. 86 (2022) 106047, https://doi.org/10.1016/j.ultsonch.2022.106047.
[46] N.K. Mahanti, S.K. Chakraborty, A. Sudhakar, D.K. Verma, S. Shankar, M. Thakur, S. Singh, S. Tripathy, A.K. Gupta, P.P. Srivastav, Refractance WindowTM-drying vs. other drying methods and effect of different process parameters on quality of foods: a comprehensive review of trends and technological developments, Future Foods 3 (2021) 100024, https://doi.org/10.1016/j.fufo.2021.100024.
[47] R. Preethi, D. Shweta, J.A. Moses, C. Anandharamakrishnan, Conductive hydro drying as an alternative method for egg white powder production, Drying Technol. 39 (2021) 324–336, https://doi.org/10.1080/07373937.2020.1788073.
[48] E.E. Özdemir, A. Görgüç, E. Gençdağ, F.M. Yılmaz, Physicochemical, functional and emulsifying properties of plant protein powder from industrial sesame processing waste as affected by spray and freeze drying, LWT 154 (2022) 112646, https://doi.org/10.1016/j.lwt.2021.112646.
[49] O.A. Caparino, J. Tang, C.I. Nindo, S.S. Sablani, J.R. Powers, J.K. Fellman, Effect of drying methods on the physical properties and microstructures of mango (Philippine 'Carabao' var.) powder, J. Food Eng. 111 (2012) 135–148, https://doi.org/10.1016/j.jfoodeng.2012.01.010.
[50] H. Du, J. Zhang, S. Wang, A. Manyande, J. Wang, Effect of high-intensity ultrasonic treatment on the physicochemical, structural, rheological, behavioral, and foaming properties of pumpkin (Cucurbita moschata Duch.)-seed protein isolates, LWT 155 (2022) 112952, https://doi.org/10.1016/j.lwt.2021.112952.
[51] H. Jin, S. Sun, Z. Sun, Q. Wang, Y. Jin, L. Sheng, Ultrasonic-assisted spray drying as a tool for improving the instant properties of egg white powder, Food Struct. 33 (2022) 100289, https://doi.org/10.1016/j.foostr.2022.100289.
[52] Z. Ma, Y. Chi, H. Zhang, Y. Chi, Y. Ma, Inhibiting effect of dry heat on the heat-induced aggregation of egg white protein, Food Chem. 387 (2022), https://doi.org/10.1016/j.foodchem.2022.132850.
[53] Z. Wang, Y. Li, L. Jiang, B. Qi, L. Zhou, Relationship between secondary structure and surface hydrophobicity of soybean protein isolate subjected to heat treatment, J. Chem. 2014 (2014), https://doi.org/10.1155/2014/475389.
[54] J.S. Cobb, V. Zai-Rose, J.J. Correia, A.V. Janorkar, FT-IR spectroscopic analysis of the secondary structures present during the desiccation induced aggregation of elastin-like polypeptide on silica, ACS Omega 5 (2020) 8403–8413, https://doi.org/10.1021/acsomega.0c00271.
[55] S. Lee, S. Han, K. Jo, S. Jung, The impacts of freeze-drying-induced stresses on the quality of meat and aquatic products: mechanisms and potential solutions to acquire high-quality products, Food Chem. 459 (2024), https://doi.org/10.1016/j.foodchem.2024.140437.
[56] J.F.A. Perlitz, L. Gentner, P.A.B. Braeuer, S. Will, Measurement of secondary structure changes in poly-L-lysine and lysozyme during acoustically levitated single droplet drying experiments by in situ raman spectroscopy, Sensors 22 (2022), https://doi.org/10.3390/s22031111.
[57] G. Karabulut, H. Feng, O. Yemiş, Physicochemical and antioxidant properties of industrial hemp seed protein isolate treated by high-intensity ultrasound, Plant Foods Hum. Nutr. 77 (2022) 577–583, https://doi.org/10.1007/s11130-022-01017-7.
[58] W. Katekhong, S. Charoenrein, Changes in physical and gelling properties of freeze-dried egg white as a result of temperature and relative humidity, J. Sci. Food Agric. 96 (2016) 4423–4431, https://doi.org/10.1002/jsfa.7653.
[59] Q. Rao, T.P. Labuza, Effect of moisture content on selected physicochemical properties of two commercial hen egg white powders, Food Chem. 132 (2012) 373–384, https://doi.org/10.1016/j.foodchem.2011.10.107.
[60] S. Ma, S. Zhao, Y. Zhang, Y. Yu, J. Liu, M. Xu, Quality characteristic of spray-drying egg white powders, Mol. Biol. Rep. 40 (2013) 5677–5683, https://doi.org/10.1007/s11033-013-2669-1.
[61] S. Martini, R. Potter, M.K. Walsh, Optimizing the use of power ultrasound to decrease turbidity in whey protein suspensions, Food Res. Int. 43 (2010) 2444–2451, https://doi.org/10.1016/j.foodres.2010.09.018.
[62] L. Li, Y. Zhou, F. Teng, S. Zhang, B. Qi, C. Wu, T. Tian, Z. Wang, Y. Li, Application of ultrasound treatment for modulating the structural, functional and rheological properties of black bean protein isolates, Int. J. Food Sci. Technol. 55 (2020) 1637–1647, https://doi.org/10.1111/ijfs.14428.
[63] M. Friedman, Improvement in the safety of foods by sulfhydryl-containing amino acids and peptides. A review, J. Agric. Food Chem. 42 (1994) 3–20, https://doi.org/10.1021/jf00037a002.
[64] Y. Mine, Recent advances in the understanding of egg white protein functionality, Trends Food Sci. Technol. 6 (1995) 225–232, https://doi.org/10.1016/S0924-2244(00)89083-4.
[65] R.-X. Yang, W.-Z. Li, C.-Q. Zhu, Q. Zhang, Effects of ultra-high hydrostatic pressure on foaming and physical-chemistry properties of egg white, J. Biomed. Sci. Eng. 02 (2009) 617–620, https://doi.org/10.4236/jbise.2009.28089.
[66] G. Karabulut, G. Goksen, A. Mousavi Khaneghah, Plant-based protein modification strategies towards challenges, J. Agric. Food Res. 15 (2024), https://doi.org/10.1016/j.jafr.2024.101017.
[67] A.R. Jambrak, T.J. Mason, V. Lelas, L. Paniwnyk, Z. Herceg, Effect of ultrasound treatment on particle size and molecular weight of whey proteins, J. Food Eng. 121 (2014) 15–23, https://doi.org/10.1016/j.jfoodeng.2013.08.012.